U.S. DEPARTMENT OF ENERGY | Office of Science

DOE/SC-ARM-TR-287

SAIL Field Campaign X-Band Precipitation Radar Surface Quantitative Precipitation Estimation (SQUIRE) Value-Added Product Report

MA Grover
RC Jackson
SM Collis
A Theisen
D Feldman
JR O'Brien
ZS Sherman
BA Raut
M Tuftedal

April 2023

ARM

DISCLAIMER

DOE/SC-ARM-TR-287

SAIL Field Campaign X-Band Precipitation Radar Surface Quantitative Precipitation Estimation (SQUIRE) Value-Added Product Report

MA Grover, Argonne National Laboratory (ANL)
Principal Investigator

JR O'Brien, ANL
RC Jackson, ANL
ZS Sherman, ANL
SM Collis, ANL
BA Raut, Northwestern University
A Theisen, ANL
M Tuftedal, ANL
D Feldman, Lawrence Berkeley National Laboratory
Co-Investigators

April 2023

How to cite this document:

Grover, MA, JR O'Brien, RC Jackson, ZS Sherman, SM Collis BA Raut, A Theisen, M Tuftedal, and D Feldman. 2023. SAIL Field Campaign X-Band Precipitation Radar Surface Quantitative Precipitation Estimation (SQUIRE) Value-Added Product Report. U.S. Department of Energy, Atmospheric Radiation Measurement user facility, Richland, Washington. DOE/SC-ARM-TR-287.

Work supported by the U.S. Department of Energy,
Office of Science, Office of Biological and Environmental Research

Executive Summary

In 2010, the U.S. Department of Energy Atmospheric Radiation Measurement (ARM) user facility procured 3- and 5-cm wavelength radars for documenting the macrophysical, microphysical, and dynamical structure of precipitating systems. In order to maximize the scientific impact, ARM supported the development of an application chain to correct for various phenomena in order to retrieve the lowest retrieved value on a Cartesian grid. This report details the motivation, science, and progress to date, as well as charting a path forward.

Acknowledgments

This work would not have been possible without the support and patience of the scientific community.

Acronyms and Abbreviations

ANL	Argonne National Laboratory
ARM	Atmospheric Radiation Measurement
CACTI	Cloud, Aerosol, and Complex Terrain Interactions
CMAC	Corrected Moments in Antenna Coordinates
CSU	Colorado State University
Py-ART	Python ARM Radar Toolkit
QPE	quantitative precipitation estimate
RELAMPAGO	Remote Sensing of Electrification, Lightning, and Mesoscale/Microscale Processes with Adaptive Ground Observations
SAIL	Surface Atmosphere Integrated Field Laboratory
SQUIRE	Surface Quantitative Precipitation Estimation
VAP	value-added product

Contents

Figures

Tables

1.0 Introduction

The U.S. Department of Energy Atmospheric Radiation Measurement (ARM) user facility has a long history of deploying precipitation weather radars. These precipitation radars scan across various azimuths and elevations, collecting precipitation characteristics across a wide domain (typically on the order of a couple of hundred kilometers from the radar site). Weather radar data are collected in native antenna coordinates, with dimensions azimuth (angle from degrees north, rotating clockwise around the radar), and range (distance from the radar). These data dimensions can make it difficult to directly compare to data on Cartesian grids (ex. x, y or latitude, longitude). One of the first data transformations users usually apply is mapping radar data from antenna to Cartesian coordinates, which is one of the most used features in the Python ARM Radar Toolkit (Py-ART; Helmus and Collis 2017).

The Surface Atmosphere Integrated Field Laboratory (SAIL) field campaign near Crested Butte, Colorado offers a unique challenge − large variations in terrain height around the radar. The radar beam is often blocked by mountains, which can create challenges when working with data. Surface Quantitative Precipitation Estimation (SQUIRE) combines the antenna-to-Cartesian data transformation, as well as extracting the lowest gate available for each grid cell in the domain. This provides data fields on a grid that modelers or other scientists can add to their analysis, including surface estimates of liquid precipitation.

2.0 Data Processing Workflow

The SQUIRE product makes use of another ARM value-added product (VAP), Corrected Moments in Antenna Coordinates (CMAC). The CMAC data are used as input for the gridding algorithm.

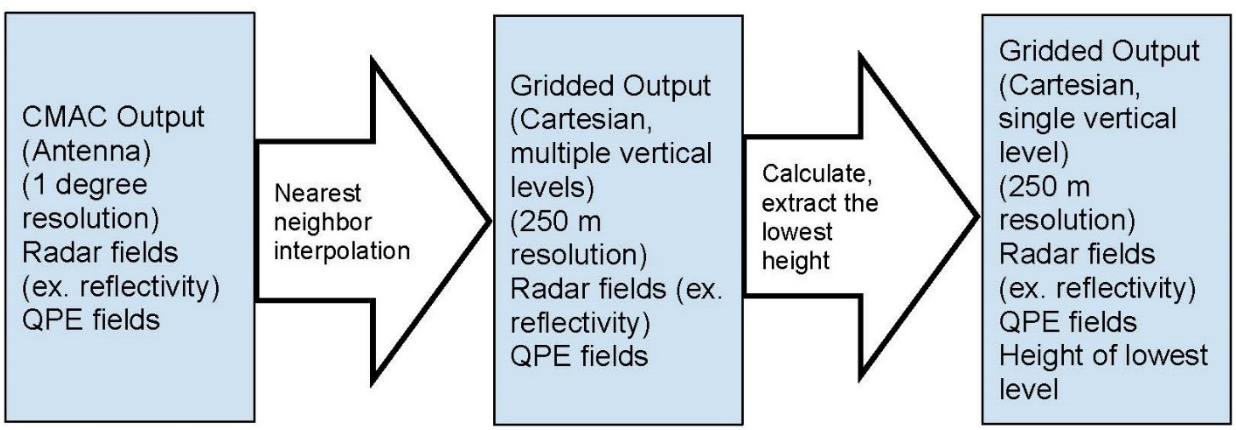

Figure 1. SQUIRE workflow, transforming CMAC data with quantitative precipitation estimate (QPE) fields to a gridded product valid at the lowest vertical level at each point.

2.1 CMAC Output

2.1.1 Colorado State University (CSU) X-Band Radar Moments

The core radar moment used in this VAP is the horizontal reflectivity field, provided by the CMAC output. This reflectivity field was corrected for attenuation and beam blockage, resulting in a clean field for use within this product. For a more detailed description of the radar moments available in the X-band radar near the SAIL site, read the CMAC technical document.

2.1.2 Snow QPE Fields

The CMAC data include liquid equivalent from snowfall estimates, using a variety of empirical relationships represented by the equivalent radar reflectivity factor (Z_e) to liquid-equivalent snowfall rates ($Z_e = aS^b$) relationship, described in Section 2.5 of the CMAC XPRECIPRADAR technical document (O'Brien et al. 2023). A summary of the relationships used are described in Table 1.

Table 1. Empirical relationships used to calculate estimated snowfall rates from radar.

Source	Z(S)	A coefficient	B coefficient	Rada band
Wolfe and Snider (2012)	$Z = 110S^2$	110	2	S
WSR-88D High Plains	$Z = 130S^2$	130	2	S
Braham (1990) 1	$Z = 67S^{1.28}$	67	1.28	X
Braham (1990) 2	$Z = 114S^{1.39}$	114	1.39	X

These values, as with the radar moments, are in the native antenna coordinates. An example of the reflectivity and snowfall field (using the Braham [1990] 1 relationship) is shown in Figure 2.

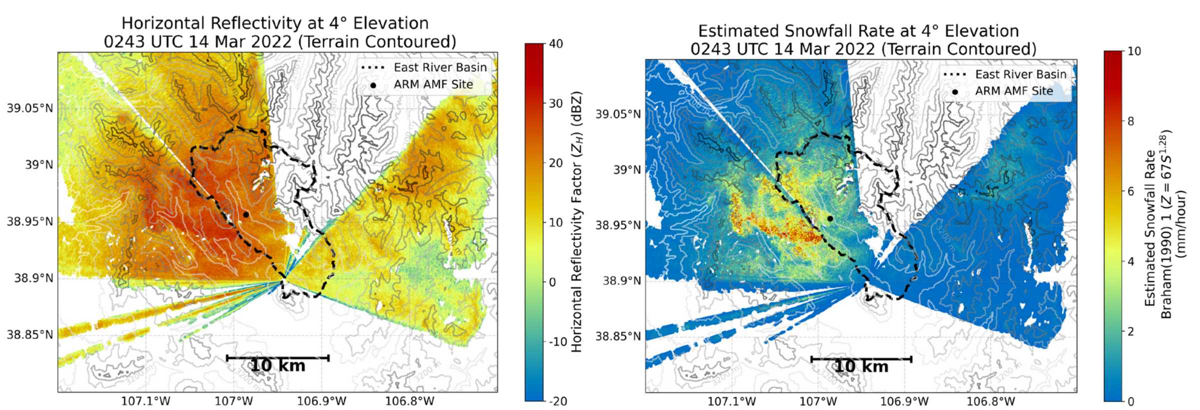

Figure 2. Horizontal reflectivity (left) and estimated QPE from snow (right) at 4 degrees elevation using the Braham (1990) 1 Z(S) relationship.

2.2 Transformation to a Cartesian Grid

When mapping from antenna coordinates to Cartesian coordinates, there are a variety of gridding algorithms to choose from. In this case, we chose the nearest-neighbor interpolation routine. The gridding parameters are provided in Table 2.

Table 2. Cartesian gridding algorithm and domain parameters.

Domain horizontal extent (x direction by y direction)	Domain vertical extent	Horizontal resolution	Vertical resolution	Gridding routine	Radius of influence
40 km x 40 km	5 km	250 m	250 m	Nearest neighbor	250 m

2.3 Locating the Surface

One of the challenges this product attempts to overcome is representing precipitation characteristics around terrain. More specifically, which vertical level to choose? If one decides to use the lowest vertical level in the domain (250 meters above ground level), terrain enhanced or even blocked regions are excluded. An example of the terrain complexity and its impact on the radar is shown in Figure 3.

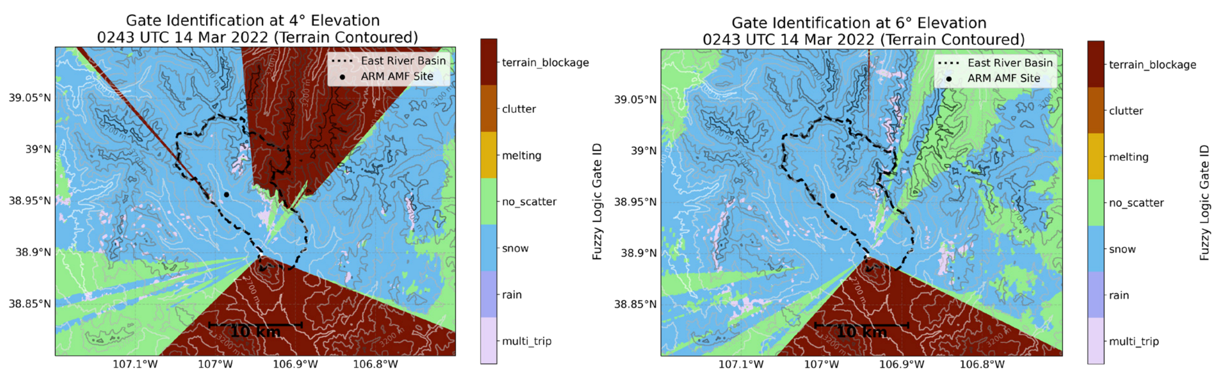

Figure 3. Gate identification, as determined by the fuzzy logic algorithm implemented in CMAC, with the 4-degree elevation (left) and the 6-degree elevation (right) plotted.

We attempt to deal with this complexity by reducing it to a horizontal domain (latitude, longitude), where the lowest vertical level, not blocked by terrain, is selected at each grid cell. An example of the lowest vertical level for a given grid is shown in Figure 4. Notice how higher terrain, and distance from the radar, require higher vertical levels.

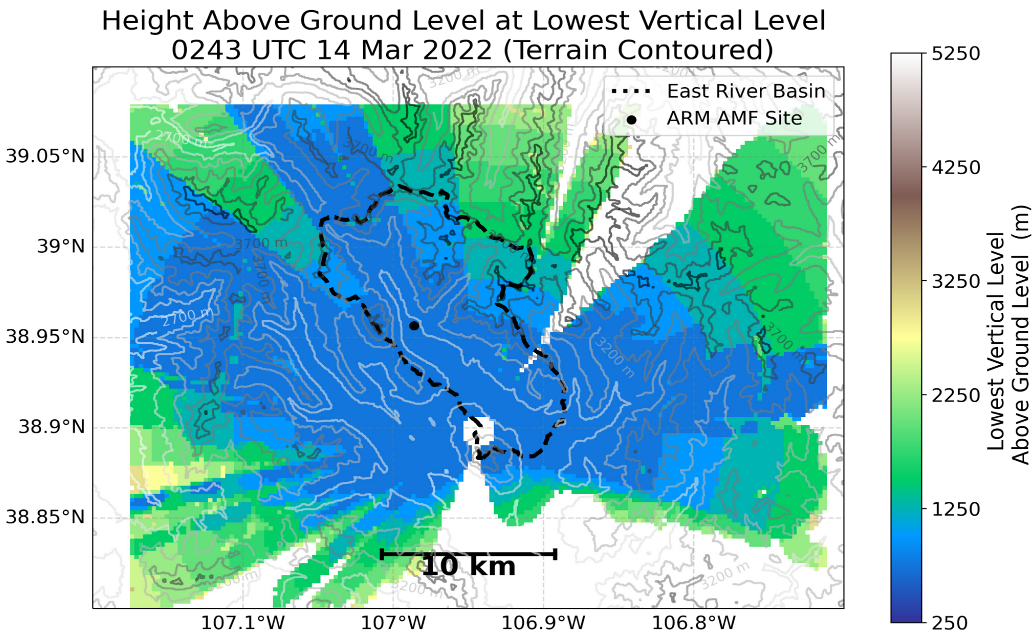

Figure 4. The lowest vertical level for each grid cell, with the SAIL domain and terrain contoured. For much of the East River Basin, the lowest vertical level is near a few hundred meters, but due to the terrain, the eastern portion of the terrain requires values from higher elevations.

These vertical levels are used to subset the grid, reducing the dimensionality from three dimensional (height above ground level, latitude, longitude) to two dimensional (latitude, longitude). The corrected horizontal reflectivity, QPE fields, and lowest vertical level are provided in the output. An example of one of the snowfall QPE fields is provided in Figure 5.

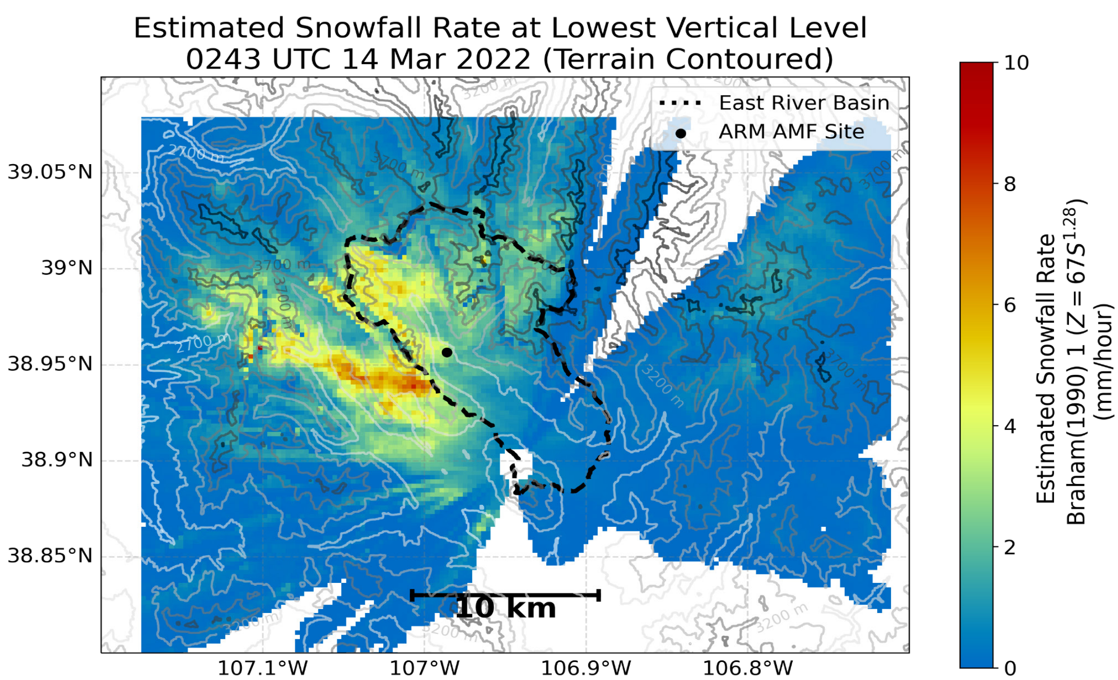

Figure 5. Example snowfall rate field, valid at the lowest vertical level.

3.0 Challenges

Analyzing remotely sensed precipitation fields near terrain is an inherently challenging task. The radar beam can be contaminated by mountains, trees, or other objects. There is also a high amount of uncertainty when estimating liquid precipitation from snow, as is mentioned in the CMAC technical document. This is a best-estimate product, using the terrain, precipitation, and scientific information available.

4.0 Future Work

Currently, reflectivity and snowfall rates are projected from the lowest valid elevation to the surface without correcting for the change in reflectivity factor with height. Future work will look at the change of reflectivity factor with height from the Ka-band ARM Zenith Radar and the radar inputs to SQUIRE and correct for this.

A similar methodology would be helpful when looking at rainfall around complex terrain, including the Remote Sensing of Electrification, Lightning, and Mesoscale/Microscale Processes with Adaptive Ground Observations (RELAMPAGO)-Cloud, Aerosol, and Complex Terrain Interactions (CACTI) campaign in the Sierras de Córdoba region of Argentina.

Furthermore, as improvements are made to CMAC fields, such as gate-ID, SQUIRE will be updated to reflect these improvements.

5.0 References

Al-Sakka, H, AA Boumahmoud, B Fradon, SJ Frasier, and P Tabary. 2013. "A New Fuzzy Logic Hydrometeor Classification Scheme Applied to the French X-, C-, and S-Band Polarimetric Radars." *Journal of Applied Meteorology and Climatology* 52(10): 2328–2344, https://doi.org/10.1175/JAMC-D-12-0236.1

Bringi, VN, GJ Huang, V Chandrasekar, and E Gorgucci. 2002. "A Methodology for Estimating the Parameters of a Gamma Raindrop Size Distribution Model from Polarimetric Radar Data: Application to a Squall-Line Event from the TRMM/Brazil Campaign." *Journal of Atmospheric and Oceanic Technology* 19(5): 633–645, https://doi.org/10.1175/1520-0426(2002)019<0633:AMFETP>2.0.CO;2

Dolan, B, and SA Rutledge. 2009. "A Theory-Based Hydrometeor Identification Algorithm for X-Band Polarimetric Radars." *Journal of Atmospheric and Oceanic Technology* 26(10): 2071–2088, https://doi.org/10.1175/2009JTECHA1208.1

Du, P, WA Kibbe, and SM Lin. 2006. "Improved peak detection in mass spectrum by incorporating continuous wavelet transform-based pattern matching." *Bioinformatics* 22(17): 2059–2065, https://doi.org/10.1093/bioinformatics/btl355

Gaustad, K, T Shippert, B Ermold, S Beus, J Daily, A Borsholm, and K Fox. 2014. "A scientific data processing framework for time series netcdf data." *Environmental Modelling & Software* 60: 241–249, https://doi.org/10.1016/j.envsoft.2014.06.005

Giangrande, SE, and AV Ryzhkov. 2008. “Estimation of rainfall based on the results of polarimetric echo classification.” *Journal of Applied Meteorology and Climatology* 47(9): 2445–2462, https://doi.org/10.1175/2008JAMC1753.1

Giangrande, SE, R McGraw, and L Lei. 2013. “An Application of Linear Programming to Polarimetric Radar Differential Phase Processing.” *Journal of Atmospheric and Oceanic Technology* 30(8): 1716–1729, https://doi.org/10.1175/JTECH-D-12-00147.1

Gourley, JJ, P Tabary, and J Parent du Chatelet. 2007. “A Fuzzy Logic Algorithm for the Separation of Precipitating from Nonprecipitating Echoes Using Polarimetric Radar Observations.” *Journal of Atmospheric and Oceanic Technology* 24(8): 1439–1451, https://.doi.org/10.1175/JTECH2035.1

Gu, JY, A Ryzhkov, P Zhang, P Neilley, M Knight, B Wolf, and DI Lee. 2011. “Polarimetric Attenuation Correction in Heavy Rain at C Band.” *Journal of Applied Meteorology and Climatol*ogy 50(1): 39–58, https://doi.org/10.1175/2010JAMC2258.1

Heistermann, M, S Collis, MJ Dixon, S Giangrande, JJ Helmus, B Kelley, J Koistinen, DB Michelson, M Peura, T Pfaff, and DB Wolff. 2014. “The Emergence of Open-Source Software for the Weather Radar Community.” *Bulletin of the American Meteorological Society* 96(1): 117−128, https://doi.org/10.1175/BAMS-D-13-00240.1

Helbush, RE. 1968. “Linear programming applied to operational decision making in weather risk situations.” *Monthly Weather Review* 96(12): 876–882, https://doi.org/10.1175/1520-0493(1968)096<0876:LPATOD>2.0.CO;2

Helmus, JJ, and SM Collis. 2016. “The Python ARM Radar Toolkit (Py-ART), a library for working with weather radar data in the Python programming language.” *Journal of Open Research Software* 4(1): e25, https://doi.org/10.5334/jors.119

James, CN, and RA Houze. 2001. “A Real-Time Four-Dimensional Doppler Dealiasing Scheme.” *Journal of Atmospheric and Oceanic Technology* 18(10): 1674–1683, https://doi.org/10.1175/1520-0426(2001)018<1674:ARTFDD>2.0.CO;2

Jones, E, T Oliphant, and P Peterson. 2001. SciPy: Open source scientific tools for Python. https://www.scipy.org/, [Online; accessed 2016-03-02].

Kollias, P, l Jo, P Borque, A Tatarevic, K Lamer, N Bharadwaj, K Widener, K Johnston, and EE Clothiaux. 2013. “Scanning ARM Cloud Radars. Part II: Data Quality Control and Processing.” *Journal of Atmospheric and Oceanic Technology* 31(3): 583–598, https://doi.org/10.1175/JTECH-D-13-00045.1

Mather, JH, and JW Voyles. 2012. “The Arm Climate Research Facility: A Review of Structure and Capabilities.” *Bulletin of the. American Meteorological Society* 94(3): 377–392, https://doi.org/10.1175/BAMS-D-11-00218.1

O'Brien, JR, M Grover, RC Jackson, ZS Sherman, SM Collis, A Theisen, BA Raut, M Tuftedal, and D Feldman. 2023. Colorado State University (CSU) X-Band Precipitation Radar Plan Position Indicator Data Processed with Corrected Moments in Antenna Coordinates (CMAC) Technical Report. U.S. Department of Energy.

Varble, A, S Nesbitt, P Salio, E Avila, P Borque, P DeMott, G McFarquhar, S van den Heever, E Zipser, D Gochis, R Houze, M Jensen, P Kollias, S Kreidenweis, R Leung, K Rasmussen, D Romps, and C Williams. 2019. Cloud, Aerosol, and Complex Terrain Interactions (CACTI) Field Campaign Report. U.S. Department of Energy. DOE/SC-ARM-19-028, https://doi.org/10.2172/1574024

Wen, G, A Protat, PT May, X Wang, and W Moran. 2015. "A Cluster-Based Method for Hydrometeor Classification Using Polarimetric Variables. Part I: Interpretation and Analysis." *Journal of Atmospheric and Oceanic Technology* 32(7): 1320–1340, https://doi.org/10.1175/JTECH-D-13-00178.1

Wikipedia, the free encyclopedia. 2016. Directional statistics. https://en.wikipedia.org/w/index.php?title=Directionalstatistics&oldid=705952853, [Online; accessed 1-March-2016].

Appendix A

Output Data

```
netcdf SAIL_SQUIRE_DOD_v1 {
dimensions:
        time = 1 ;
        y = 161 ;
        x = 161 ;
variables:
        int64 time(time) ;
                time:long_name = "Time in Seconds from Volume Start" ;
                time:calendar = "standard" ;
                time:standard_name = "time" ;
        int64 y(y) ;
                y:long_name = "Y distance on the projection plane from the origin" ;
                y:units = "m" ;
                y:standard_name = "projection_y_coordinate" ;
                y:axis = "Y" ;
        int64 x(x) ;
                x:long_name = "X distance on the projection plane from the origin" ;
                x:units = "m" ;
                x:standard_name = "projection_x_coordinate" ;
                x:axis = "X" ;
```

```
double DBZ(time, y, x) ;
        DBZ:_FillValue = -32768. ;
        DBZ:long_name = "Equivalent Radar Reflectivity Factor" ;
        DBZ:units = "dBZ" ;
        DBZ:standard_name = "equivalent_reflectivity_factor" ;
        DBZ:coordinates = "lat z lon" ;
double corrected_reflectivity(time, y, x) ;
        corrected_reflectivity:_FillValue = 1.e+20 ;
        corrected_reflectivity:long_name = "Corrected reflectivity" ;
        corrected_reflectivity:units = "dBZ" ;
        corrected_reflectivity:standard_name = "corrected_equivalent_reflectivity_factor" ;
        corrected_reflectivity:coordinates = "lat z lon" ;
double rain_rate_A(time, y, x) ;
        rain_rate_A:_FillValue = 1.e+20 ;
        rain_rate_A:long_name = "Rainfall Rate from Specific Attenuation" ;
        rain_rate_A:units = "mm/hr" ;
        rain_rate_A:comment = "Rain rate calculated from specific_attenuation,
R=43.5*specific_attenuation**0.79, note R=0.0 where norm coherent power < 0.4 or rhohv < 0.8" ;
        rain_rate_A:valid_min = "0.0" ;
        rain_rate_A:valid_max = "400.0" ;
        rain_rate_A:coordinates = "elevation azimuth range" ;
        rain_rate_A:standard_name = "rainfall_rate" ;
double snow_rate_ws88diw(time, y, x) ;
        snow_rate_ws88diw:_FillValue = 1.e+20 ;
        snow_rate_ws88diw:long_name = "Snowfall rate from Z using WSR 88D High Plains" ;
        snow_rate_ws88diw:units = "mm/h" ;
        snow_rate_ws88diw:standard_name = "snowfall_rate" ;
```

```
                snow_rate_ws88diw:coordinates = "lat z lon" ;
                snow_rate_ws88diw:valid_min = "0" ;
                snow_rate_ws88diw:valid_max = "500" ;
                snow_rate_ws88diw:swe_ratio = "13.699" ;
                snow_rate_ws88diw:A = "40" ;
                snow_rate_ws88diw:B = "2" ;
        double snow_rate_m2009_1(time, y, x) ;
                snow_rate_m2009_1:_FillValue = 1.e+20 ;
                snow_rate_m2009_1:long_name = "Snowfall rate from Z using Matrosov et al.(2009)
Braham(1990) 1" ;
                snow_rate_m2009_1:units = "mm/h" ;
                snow_rate_m2009_1:standard_name = "snowfall_rate" ;
                snow_rate_m2009_1:coordinates = "lat z lon" ;
                snow_rate_m2009_1:valid_min = "0" ;
                snow_rate_m2009_1:valid_max = "500" ;
                snow_rate_m2009_1:swe_ratio = "13.699" ;
                snow_rate_m2009_1:A = "67" ;
                snow_rate_m2009_1:B = "1.28" ;
        double snow_rate_m2009_2(time, y, x) ;
                snow_rate_m2009_2:_FillValue = 1.e+20 ;
                snow_rate_m2009_2:long_name = "Snowfall rate from Z using Matrosov et al.(2009)
Braham(1990) 2" ;
                snow_rate_m2009_2:units = "mm/h" ;
                snow_rate_m2009_2:standard_name = "snowfall_rate" ;
                snow_rate_m2009_2:coordinates = "lat z lon" ;
                snow_rate_m2009_2:valid_min = "0" ;
                snow_rate_m2009_2:valid_max = "500" ;
                snow_rate_m2009_2:swe_ratio = "13.699" ;
```

snow_rate_m2009_2:A = "114" ;

snow_rate_m2009_2:B = "1.39" ;

double snow_rate_ws2012(time, y, x) ;

snow_rate_ws2012:_FillValue = 1.e+20 ;

snow_rate_ws2012:long_name = "Snowfall rate from Z using Wolf and Snider (2012)" ;

snow_rate_ws2012:units = "mm/h" ;

snow_rate_ws2012:standard_name = "snowfall_rate" ;

snow_rate_ws2012:coordinates = "lat z lon" ;

snow_rate_ws2012:valid_min = "0" ;

snow_rate_ws2012:valid_max = "500" ;

snow_rate_ws2012:swe_ratio = "13.699" ;

snow_rate_ws2012:A = "110" ;

snow_rate_ws2012:B = "2" ;

double z(time, y, x) ;

z:_FillValue = NaN ;

z:long_name = "Z distance on the projection plane from the origin" ;

z:units = "m" ;

z:standard_name = "projection_z_coordinate" ;

z:axis = "Z" ;

z:positive = "up" ;

double lowest_height(time, y, x) ;

lowest_height:_FillValue = -9999.9 ;

lowest_height:long_name = "Height of the lowest Radar Gate" ;

lowest_height:units = "m" ;

lowest_height:coordinates = "lat z lon" ;

lowest_height:standard_name = "height" ;

double lat(y) ;

lat:_FillValue = NaN ;

lat:long_name = "North latitude" ;

lat:units = "degree_N" ;

lat:standard_name = "latitude" ;

lat:valid_min = "-90" ;

lat:valid_max = "90" ;

double lon(x) ;

lon:_FillValue = NaN ;

lon:long_name = "East longitude" ;

lon:units = "degree_E" ;

lon:standard_name = "longitude" ;

lon:valid_min = "-180" ;

lon:valid_max = "180" ;

// global attributes:

:command_line = "" ;

:Conventions = "ARM-1.3 CF/Radial instrument_parameters" ;

:process_version = "" ;

:dod_version = "" ;

:site_id = "" ;

:platform_id = "" ;

:facility_id = "" ;

:data_level = "" ;

:location_description = "" ;

:datastream = "" ;

:institution = "U.S. Department of Energy Atmospheric Radiation Measurement (ARM) Climate Research Facility" ;

:references = "See XPRECIPRADAR Instrument Handbook" ;

:doi = "10.5439/1884979" ;

:comment = "This is highly experimental and initial data. There are many known and unknown issues. Please do not use before contacting the Translator responsible scollis@anl.gov" ;

:attributions = "This data is collected by the ARM Climate Research facility. Radar system is operated by the radar engineering team radar@arm.gov and the data is processed by the precipitation radar products team. LP code courtesy of Scott Giangrande BNL." ;

:known_issues = "False phidp jumps in insect regions. Still uses old Giangrande code. Issues with some snow below melting layer." ;

:developers = "Maxwell Grover, ANL. Joseph O\'Brien, ANL. Robert Jackson, ANL. Zachary Sherman, ANL." ;

:translator = "https://www.arm.gov/capabilities/instruments/xprecipradar" ;

:mentors = "https://www.arm.gov/connect-with-arm/organization/instrument-mentors/list#xprecipradar" ;

:source = "Colorado State University\'s X-Band Precipitation Radar (XPRECIPRADAR) (DOI: 10.5439/1844501)" ;

:input_datastreams = "xprecipradarcmacppi.c1" ;

:fields = "DBZ, corrected_reflectivity, time, lowest_height, rain_rate_A, snow_rate_ws88diw, snow_rate_m2009_1, snow_rate_m2009_2, snow_rate_ws2012, z, y, x, lat, lon" ;

:history = "" ;

}

www.arm.gov

U.S. DEPARTMENT OF ENERGY

Office of Science